Understanding Persistent Luminescence: Rare-Earth- and Eu^{2+}-doped $Sr_2MgSi_2O_7$

Mika Lastusaari[a,b], Högne Jungner[c], Aleksei Kotlov[d], Taneli Laamanen[a,b], Lucas C. V. Rodrigues[a,e], Hermi F. Brito[e], and Jorma Hölsä[a,b,e]

[a] University of Turku, Department of Chemistry, FI-20014 Turku, Finland
[b] Turku University Centre for Materials and Surfaces (MatSurf), Turku, Finland
[c] University of Helsinki, Dating Laboratory, FI-00014 Helsinki, Finland
[d] Deutsches Elektronen-Synchrotron, A Research Centre of the Helmholtz Association, Notkestrasse 85, D-22607 Hamburg, Germany
[e] Universidade de São Paulo, Instituto de Química, Av. Prof. Lineu Prestes, 748, BR-05508-000, São Paulo-SP, Brazil

Reprint requests to Prof. Dr.-Ing. Jorma Hölsä. Fax: +358-2-3336730. E-mail: jholsa@utu.fi, or Dr. Mika Lastusaari. Fax: +358-2-3336730. E-mail: miklas@utu.fi

Z. Naturforsch. **2014**, *69b*, 171 – 182 / DOI: 10.5560/ZNB.2014-3322
Received December 6, 2013

Similar to many other Eu^{2+},RE^{3+}-co-doped persistent luminescence materials, for $Sr_2MgSi_2O_7$:Eu^{2+},RE^{3+} the initial intensity and duration of persistent luminescence was also found to depend critically on the rare-earth (*RE*) co-doping. An enhancement of 1 – 2 orders of magnitude in these properties could be obtained by Dy^{3+} co-doping whereas total quenching of persistent luminescence resulted from the use of Sm^{3+} and Yb^{3+}. To solve this drastic disparity, the effects of the individual RE^{3+} ions were studied with thermoluminescence (TL) spectroscopy to derive information about the formation of traps storing the excitation energy. The charge compensation defects were concluded to be the origin of the complex TL glow curve structure. The tuning of the band gap of the $Sr_2MgSi_2O_7$ host and especially the position of the bottom of the conduction band due to the Eu^{2+},RE^{3+} co-doping was measured with the synchrotron radiation vacuum UV (VUV) excitation spectra of the Eu^{2+} dopant. The model based on the evolution of the band gap energy with RE^{3+} co-doping was found to explain the intensity and duration of the persistent luminescence.

Key words: Persistent Luminescence, Defects, $Sr_2MgSi_2O_7$, Eu^{2+}, Rare-Earth, Co-doping

Introduction

Broadly speaking, persistent luminescence is luminescence obtained for a long time – usually for hours – after the removal of the excitation source [1]. Systematically, persistent luminescence is a special case of thermally stimulated luminescence (TSL) at a given (constant) temperature [2]. The input energy can be in the form of visible light, UV radiation, electron or plasma beam, X- or even γ-rays – much depending on the application. Nowadays, it is recognized that the excitation (irradiation) energy is stored in defects – in intrinsic traps or in those deliberately introduced, or in both, of course [3, 4]. Since the long life time of persistent luminescence is due to trapping of energy in defects, the term to be used for the phenomenon is not phosphorescence as still used incorrectly. The two phenomena – energy storage and luminescence – are somewhat in conflict with each other since it is usually (and correctly) thought that the defect-containing host material quenches conventional luminescence. However, in persistent luminescence the energy stored in defects only delays the luminescence output from a strongly emitting center. For a good persistent luminescence material, the following three requirements must thus be fulfilled: i) efficient luminescence, ii) good storage capability and iii) absence of luminescence quenching [5].

The history of persistent luminescence goes back to ancient China some 1000 years ago, and this time

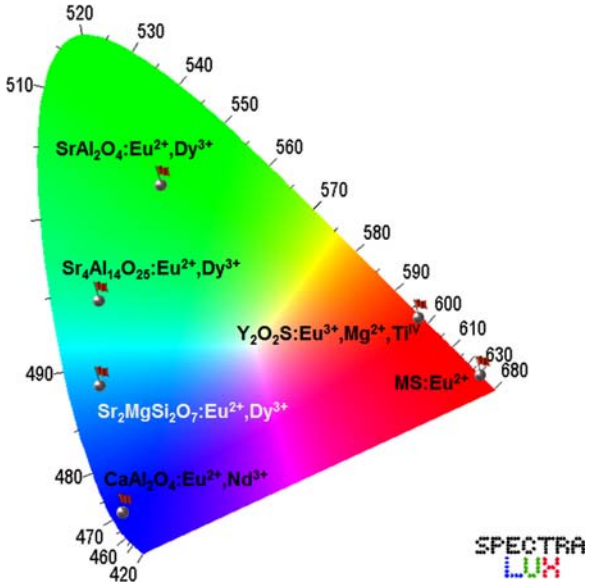

Fig. 1 (color online). The Commission Internationale de l'Éclairage (CIE) color diagram for the most efficient commercial Eu^{2+}-based (and $Y_2O_2S:Eu^{3+}$) persistent luminescence materials.

span makes persistent luminescence probably the first kind of documented luminescence [1]. However, only little is known about the materials used then. In the beginning of the 17th century, persistent luminescence certainly became the best documented kind of luminescence because of the manufacture of the famous Bologna Stone [6]. Presently, it is known that the material is Cu^{+}-doped BaS made by the reduction of the mineral Barite [7]. The driving force for the discovery of such a material was alchemy. Unfortunately, the golden color of the material did not persist significantly in daylight, and even in the dark for only a few hours.

Different persistent luminescence materials (*e. g.* copper-doped ZnS) were used since the late 19th century, but the efficiency was poor [8]. The breakthrough in the research and applications of persistent luminescence came in the mid 1990s with the introduction of the efficient Eu^{2+},RE^{3+}- (*RE*: rare-earth metal) co-doped aluminates $CaAl_2O_4:Eu^{2+},Nd^{3+}$ and $SrAl_2O_4:Eu^{2+},Dy^{3+}$ [9] emitting in the blue and green region, respectively. Presently, one can obtain any (basic) color-emitting commercial persistent luminescence material (Fig. 1), and all of them are based on divalent europium [10]. It is not difficult to imagine the reasons behind the supremacy of Eu^{2+} as the emitting center [4]: i) allowed (*i. e.* fast decay) $4f^7 \leftrightarrow 4f^6 5d^1$ transitions both in emission and excitation, ii) broad band (*i. e.* intense) emission and excitation, iii) easy tunability of emission and excitation just by changing the host (*i. e.* modification of covalency and crystal field strength) and iv) the possibility to have excitation in the visible (blue) region. Perhaps the only disadvantage in the use of Eu^{2+} is that many other luminescence applications also use europium (also as Eu^{3+}). Combined with the bulk applications and sometimes difficult recycling of the phosphors, one should in earnest seek for alternatives for Eu^{2+}/Eu^{3+}. As for the applications employing persistent luminescence materials one can cite (in no particular order): i) emergency and traffic signaling, ii) radiation detection, iii) temperature and pressure sensors, iv) textile printing and ceramics, v) solar cells, vi) food packaging, vii) medical diagnostics, and many more. Especially for medical diagnostics, red-emitting centers such as Mn^{2+} [11], Cr^{3+} [12] and perhaps Pr^{3+} [13] have been found useful due to the relative poor performance of Eu^{2+}-based materials in red. An alternative green-emitting material can be Tb^{3+} [14 – 16] as well as Ti^{3+} in blue-green [17, 18], the latter being very inexpensive though relatively inefficient.

The alkaline earth magnesium disilicate persistent luminescence phosphors, especially $Sr_2MgSi_2O_7:Eu^{2+},RE^{3+}$, have been subject to detailed investigations [19 – 51] only infrequently despite being among the most efficient phosphors of their kind. Moreover, their blue-green emission [19] corresponds better than any other phosphor to the sensitivity of the human eye in the dark [52]. Finally, despite the apparent complexity of its stoichiometry, the tetragonal $Sr_2MgSi_2O_7$ structure (Fig. 2) is very simple [53] (*e. g.* only one Sr^{2+} site) and is thus very suitable as a model compound – more than *e. g.* $SrAl_2O_4$ with a low-symmetry structure and two Sr^{2+} sites [54]. $Sr_2MgSi_2O_7$ is also very stable with no risk for decomposition *e. g.* by humidity, and thus the appearance of impurity phases is avoided. In this work, the last major source of ambiguity, the role of the RE^{3+} co-dopant in boosting the performance of the persistent luminescence materials is addressed based on both experiments, semi-empirical modelling and theoretical calculations. Up-to-date synchrotron radiation methods such as VUV spectroscopy together with thermoluminescence (TL) were used to characterize the serendipitous enhancement of the persistent luminescence intensity in the rather simple

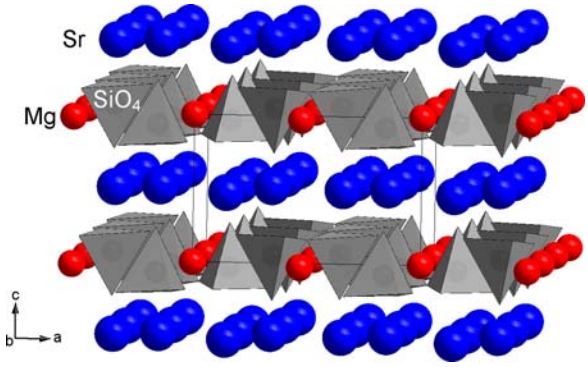

Fig. 2 (color online). The tetragonal crystal structure of $Sr_2MgSi_2O_7$.

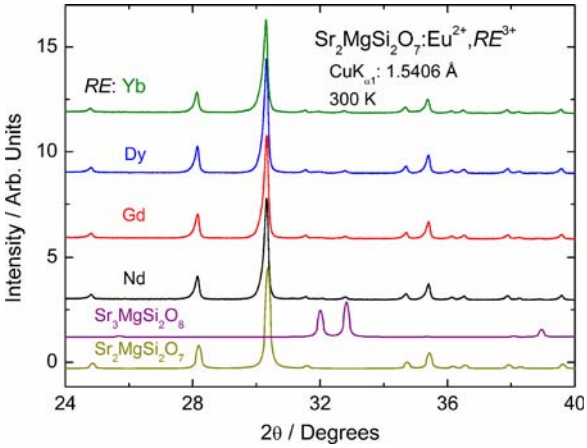

Fig. 3 (color online). The powder X-ray diffraction patterns of selected Eu^{2+},RE^{3+}-co-doped $Sr_2MgSi_2O_7$ persistent luminescence materials. The patterns for $Sr_2MgSi_2O_7$ and $Sr_3MgSi_2O_8$ [57] are given as references.

but efficient model system, the Eu^{2+},RE^{3+}-co-doped $Sr_2MgSi_2O_7$, possessing also significant commercial value.

Results and Discussion

Crystal structure and phase purity

According to the powder X-ray diffraction (PXD) patterns, the materials prepared were of the pure tetragonal $Sr_2MgSi_2O_7$ [53] phase though traces of $Sr_3MgSi_2O_8$ [57] were occasionally observed as impurities (Fig. 3). No relationship between the RE^{3+} co-doping and the amount of $Sr_3MgSi_2O_8$ could be established. No segregation of the RE_2O_3 sesquioxide or similar phases was observed probably because of the low (1 mole-%) doping level. Despite the apparently insignificant amount of the $Sr_3MgSi_2O_8$ impurity, the enriching of SrO into this phase may have important repercussions. The deficit of SrO in the $Sr_2MgSi_2O_7$ phase creates strontium and oxide vacancies which can act as hole and electron traps.

The Eu^{2+} ions are expected to occupy the Sr^{2+} site in $Sr_2MgSi_2O_7$ due to the perfect match between the ionic radii, 1.25 Å for both ions (CN: 8) [58]. Since most RE^{3+} ions are clearly smaller than Sr^{2+} (from 1.16 Å for La^{3+} to 0.98 Å for Lu^{3+} for CN: 8), they should fit into the Sr^{2+} site, too, though for the smallest RE^{3+} ions the limit for good solid solubility (size difference $<15\,\%$) given by Vegard's laws [59] is not rigorously followed. Major difficulties in solid solubility between the RE^{3+} and Sr^{2+} ions arise due to the aliovalent substitution which leads to charge compensation defects. However, the bond valence model [60] calculations have shown that the oxygen coordination around the Sr^{2+} site gives a formal valence considerably higher than 2 for this site [61]. The doping with RE^{3+} may thus be rather easy though the charge compensation problem still persists.

The tetragonal $Sr_2MgSi_2O_7$ phase belongs to the åkermanite $Ca_2MgSi_2O_7$-type structure, which in turn belongs to the much wider melilite group of minerals. The crystal structure has the space group $P\bar{4}2_1m$ (no. 113; $Z = 2$) where the Sr^{2+} ion occupies the 4*e* site with low C_s symmetry and a quite low coordination number of 8 [53, 61]. The $Sr_2MgSi_2O_7$ structure is composed of layers of corner-sharing MgO_4 and SiO_4 tetrahedra forming five-membered rings. These layers are held together by eight-coordinated Sr^{2+} cations (*cf.* Fig. 2). These structural features leave considerable free space around the Sr^{2+} site which may be needed for the charge compensation (*e. g.* interstitial oxide) due to the aliovalent substitution of Sr^{2+} by the trivalent RE^{3+}. Indeed, detailed structural studies have shown that some melilites (*e. g.* synthetic $Ca_2MgSi_2O_7$) possess a two-dimensional incommensurately modulated structure [61] to reduce structural strains caused by the misfit between layer of tetrahedra and the M^{2+} cations by a deformation of the former. It seems, however, that the particular $Sr_2MgSi_2O_7$ structure is a non-modulated one [61].

Persistent luminescence

Despite the apparent structural similarities between the different tetragonal alkaline earth disilicates ($M_2MgSi_2O_7$; *M*: Ca [62], Sr [53], Ba [63]), the persistent luminescence spectra have different features under the deep VUV excitation to the hosts' conduction band (CB) with synchrotron radiation (SR). The excellent size match between the Sr^{2+} and Eu^{2+} ions is shown in the low band width (FWHM) value for the Eu^{2+}-doped $Sr_2MgSi_2O_7$ whereas the stronger strain involved in the isovalent substitution of the much smaller Ca^{2+} ion with Eu^{2+} gives a broad band as is suggested by the differences in the ionic radii (CN: 8): 1.12 (1.42) Å for Ca^{2+} (Ba^{2+}) [58]. The strain in $Ba_2MgSi_2O_7$ seems to have a weaker effect on the persistent emission spectrum in contrast to the ionic radii.

The persistent emission spectra seem to be symmetrical excluding the possibility of several sites for the Eu^{2+} dopant in agreement with the structural data [53, 62, 63]. The position of the emission bands is not following the simple evolution although the strongest crystal field and weakest covalency in the $Ca_2MgSi_2O_7$ host results in the largest splitting of the $4f^6 5d^1$ levels and in the longest wavelength emission. On the contrary, for the position of the Eu^{2+} emission band in $Sr_2MgSi_2O_7$ and $Ba_2MgSi_2O_7$ the opposite effect is expected. The reasons for this behavior are not clear as noted already previously [64].

Since the human eye is still the most frequent detector in many persistent luminescence applications, the Eu^{2+} emission band in $Ba_2MgSi_2O_7$ gives the best match to the sensitivity of the human eye – for bright illumination conditions. However, because the persistent luminescence phosphors are used most of the time in the dark when the eye sensitivity curve moves towards the blue range [52], the position of the Eu^{2+} emission band in $Sr_2MgSi_2O_7$ is better suited.

Effect of RE^{3+} co-doping: conventional luminescence

Before going to the effect of the RE^{3+} co-doping on the persistent luminescence of Eu^{2+} in $Sr_2MgSi_2O_7$, it is worthwhile to probe the VUV-excited conventional luminescence of these materials (Fig. 4). When the RE^{3+} ions are substituted on the Sr^{2+} site, a charge compensation is necessary due to the difference in the formal valences. The most simple charge compensation scheme involves the introduction of interstitial oxide ions. In the following, the Kröger-Vink notations [65] are used.

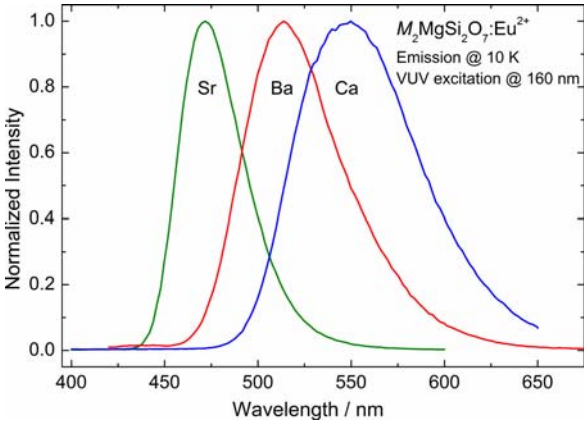

Fig. 4 (color online). The VUV-excited (at *ca.* 160 nm) emission spectra of the Eu^{2+}-doped $M_2MgSi_2O_7$ (*M*: Ca, Sr, Ba) materials at room temperature.

$$2RE^{3+} + 3O^{2-} \rightarrow 2RE^{\bullet}_{Sr} + 2O^{\times}_{o} + O''_{i} \qquad (1)$$

This scheme is the most appropriate one because of the rather open structure of the $Sr_2MgSi_2O_7$ host. Another, though a more theoretical possibility, is to balance the additional positive charge due to RE^{3+} co-doping with the formation of strontium vacancies (V''_{Sr}).

If the charge compensating defect (*e. g.* an interstitial oxide ion) is situated close to the emitting Eu^{2+} center, the difference in the crystal field effect should be reflected in the position of the Eu^{2+} emission band since the effect of the crystal field on the 5*d* orbitals is even stronger than for the more common 3*d* orbitals. The emission spectra of Eu^{2+} in $Sr_2MgSi_2O_7$ with different RE^{3+} co-doping (Fig. 5) do not reveal, however, any significant differences in band position or shape. It must thus be concluded that the RE^{3+} co-dopant and its charge compensating defect are far enough from Eu^{2+} to cause only an insignificant change in the crystal field around Eu^{2+}. In fact, there is not any direct (electrostatic) interaction between Eu^{2+} on one hand and the RE^{3+} ion or the defect on the other which would indicate that these species approach each other. In contrast, an electrostatic attraction between the $RE^{\bullet}_{Sr}$ and O''_{i} defects with opposite charges is very probable [66]. Finally, even if the additional interstitial oxide ion would enter into the proximity of Eu^{2+}, the increase in the electrostatic force around Eu^{2+} would not be excessive, only 9 oxide ions instead of 8. This observation

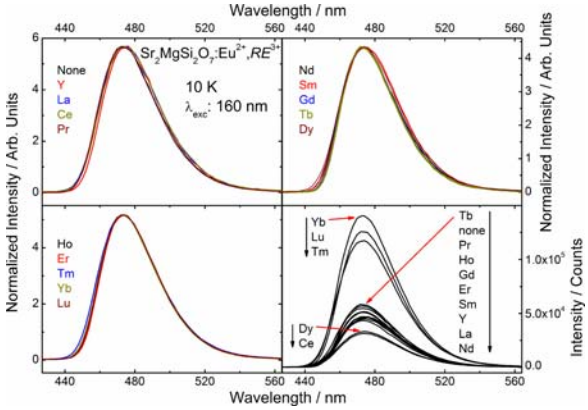

Fig. 5 (color online). The synchrotron radiation (SR) VUV-excited (time integrated) and normalized emission spectra of the $Sr_2MgSi_2O_7$:Eu^{2+},RE^{3+} (*RE*: Y, La–Lu, excl. Pm) persistent luminescence materials (counterclockwise from the upper right corner) as well as selected spectra with absolute intensities (the lower right corner) at 10 K. The excitation takes place to the conduction band of the $Sr_2MgSi_2O_7$ host at *ca.* 160 nm (SUPERLUMI, HASYLAB).

is in line with the bond valence model calculations that have shown [61] that the Sr^{2+} site has already "anticipated" the aliovalent substitution into this site by increasing the valence from the formal +2 to a higher value.

After the failure of not being able to use the Eu^{2+} ion as a structural probe to detect the charge compensating (and RE^{3+}) defects, the interest is turned to the absolute intensities of the conventional luminescence (although the measurement of these parameters is much more uncertain than that of the band positions or shapes). It is evident that there are significant differences in the conventional luminescence intensity as a function of the RE^{3+} co-doping (Fig. 5, right bottom corner). Since all these materials show persistent luminescence at room temperature, it is expected that, at the low temperature (10 K) used in these measurements, the persistent luminescence could be avoided because of the lack of sufficient thermal energy. As shown by the results this idea partly failed: the charging (but not decharging) of the defects with electrons took place at 10 K as indicated by the different decrease in the luminescence intensity. Since the beam intensity of the SR radiation in far VUV is quite low, the results confirm that the steady state condition at 10 K, *i. e.* the full charging of defects, takes a long time and the conventional luminescence remains weak for a long time – at least for the time required to measure the individual emission spectrum with the aid of a CCD detector. The charging takes more time when there are more defects explaining qualitatively the different level of intensity. When the enhancement (or quenching) of the persistent luminescence is known as a function of the RE^{3+} co-doping (see the next chapters), it would be interesting to find out if there is any quantitative relationship between the low conventional luminescence during the charging step at low temperatures and the high persistent luminescence at high temperatures.

Effect of RE^{3+} co-doping: persistent luminescence

The persistent luminescence of the Eu^{2+},Dy^{3+}-co-doped $Sr_2MgSi_2O_7$ materials could be induced by the SR VUV excitation into the $Sr_2MgSi_2O_7$ host at 160 nm. This excitation is well in the CB of the $Sr_2MgSi_2O_7$ host and relaxes then to the $4f^6 5d^1$ levels of Eu^{2+} and gives immediately most of the excitation energy as conventional luminescence. The life time of this emission is *ca.* 1 μs. Along with this emission, one observes very strong and long persistent luminescence (Fig. 6). The decay of this persistent luminescence is clearly non-exponential suggesting the presence of at least 2 or even three traps from which the bleaching of electrons with thermal energy takes different delays. The existence of more than one trap was later verified

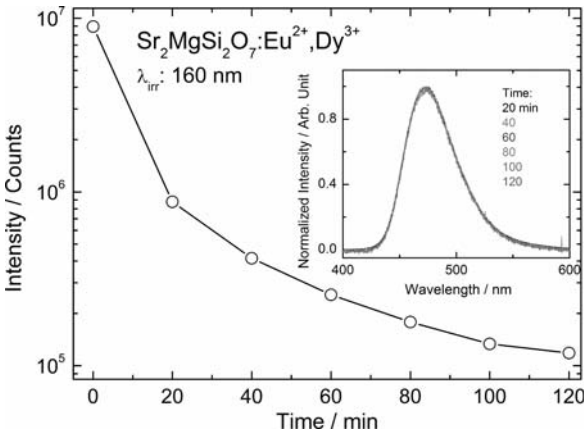

Fig. 6. The time evolution of the SR VUV-irradiated persistent luminescence intensity of the Dy^{3+} co-doped $Sr_2MgSi_2O_7$:Eu^{2+} persistent luminescence material at room temperature. Inset: the superimposed normalized persistent emission spectra of the same material.

and confirmed with the thermoluminescence measurements. It is worth noting that the persistent emission spectra are almost identical (Fig. 6; inset) which indicates that only one emitting species is present in the Eu^{2+},Dy^{3+}-co-doped $Sr_2MgSi_2O_7$ materials. This observation excludes also the possibility that the different traps feed different Eu^{2+} emitting centers and also makes inconceivable the concept that the traps are located close to the Eu^{2+} ions.

As for the main subject of this contribution, it was found that different RE^{3+} co-dopants have drastically different effects on both the initial intensity and the duration of persistent luminescence from the Eu^{2+},RE^{3+}-co-doped $Sr_2MgSi_2O_7$ materials (Fig. 7). The three "typical" RE^{3+} ions, Nd^{3+}, Dy^{3+}, and Ho^{3+}, yield by far the best persistent luminescence performance. All these "typical" ions are known to retain their 3+ oxidation state even in the most extreme conditions and are expected to do so also under VUV irradiation. The "atypical" RE^{3+} ions such as Sm^{3+} and Yb^{3+} (but evidently not Tm^{3+}) which can undergo an easy reduction to the divalent state seem to quench efficiently the persistent luminescence. This property may be related to their inability to form charge compensation defects in the divalent state. On the other hand, the Sm^{2+} and Yb^{2+} ions have very low-energy 5*d* states which may interfere with the persistent luminescence process as killer sites. Finally, the Sm^{3+}- and Yb^{3+}-co-doped $Sr_2MgSi_2O_7$:Eu^{2+} materials have been shown to possess deep traps below the bottom of the CB of $Sr_2MgSi_2O_7$ [67]. There is spectroscopic evidence (though only for Sm^{3+}-doped $SrAl_2O_4$ [68]) that at least samarium is in the divalent state and probably also ytterbium since the reduction potential of Yb^{3+} is lower than that of Sm^{3+} [69]. As a conclusion, if Sm^{2+} and Yb^{2+} ions exist in $Sr_2MgSi_2O_7$ – as is conceivable – several mechanisms can quench the persistent luminescence from $Sr_2MgSi_2O_7$:Eu^{2+}.

The other "atypical" RE^{3+} ions such as Ce^{3+}, Pr^{3+} and Tb^{3+}, which are prone to easy oxidation, cause next to no enhancement of persistent luminescence from $Sr_2MgSi_2O_7$:Eu^{2+} but they either do not quench it. The interference of the tetravalent RE^{IV} ions could be a problem with VUV irradiation, but UV irradiation at 254 nm is hard enough to cause the oxidation of these RE^{3+} ions in high band gap energy materials such as $Sr_2MgSi_2O_7$ (the E_g value is *ca.* 7.1 eV). Accordingly, these ions should be treated as belonging to the "typical" RE^{3+} ions.

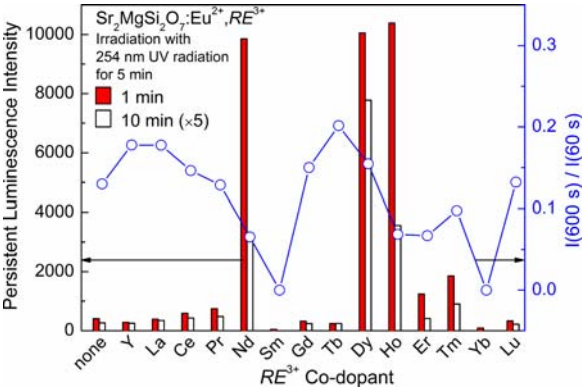

Fig. 7 (color online). The effect of RE^{3+} co-doping on the UV-irradiated (254 nm) persistent luminescence intensity of Eu^{2+} in the $Sr_2MgSi_2O_7$:Eu^{2+},RE^{3+} (*RE*: Y, La–Lu, excl. Pm) materials at room temperature with different delays (1 and 10 min) after irradiation.

There is also a group of "typical" RE^{3+} ions, Y^{3+}, La^{3+}, Gd^{3+}, and Lu^{3+}, with no effect on the persistent luminescence, as well as Er^{3+} (and Tm^{3+}) with an only slightly enhancing effect. It is very difficult if not impossible to classify the effect of these ions based on their chemical behavior. Other explanations need to be found for their inactivity or relatively weak activity in boosting the persistent luminescence from $Sr_2MgSi_2O_7$:Eu^{2+}.

In general, those RE^{3+} ions which enhance the persistent luminescence of $Sr_2MgSi_2O_7$:Eu^{2+} (Fig. 7) at room temperature show weakened conventional luminescence at 10 K, too (Fig. 5). The correspondence is not perfect, probably because the conditions (temperature) are very different.

When returning to the three "typical" RE^{3+} ions, Nd^{3+}, Dy^{3+}, and Ho^{3+}, which yield the best persistent luminescence performance (Fig. 7), one can observe important differences in the time dependence: both Nd^{3+}- and Ho^{3+}-co-doped materials experience within the first 10 min a much faster decline in the persistent luminescence intensity than the Dy^{3+}-co-doped material. The long-lasting persistent luminescence can be related to the existence of deeper traps the bleaching of which takes a long time – either *via* the CB of the host or *via* the presently much studied tunneling mechanism. In fact, the presence of deep traps with significant density for the Dy^{3+}-co-doped material was observed in a previous thermoluminescence study [67].

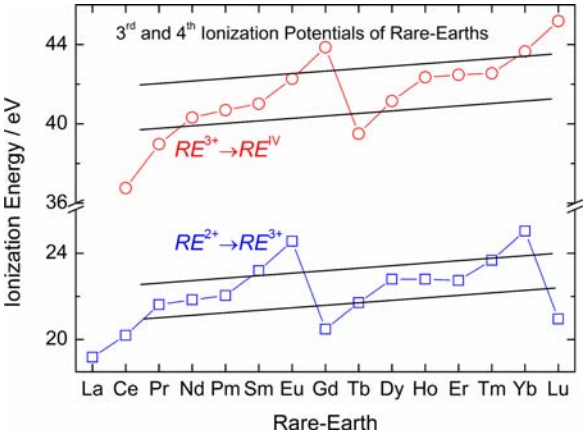

Fig. 8 (color online). The 3rd (and 4th) ionization energies [71] for the RE^{2+} (and RE^{3+}) ions.

It seems evident that the enhancement of the persistent luminescence from the Eu^{2+},RE^{3+}-co-doped $Sr_2MgSi_2O_7$ materials cannot be explained by the arguments presented earlier [70]. These arguments were based on the chemical properties of the RE^{3+} ions, the host structure, rare-earth ion size, charge density, or simple redox behavior (evidently except for Sm^{3+} and Yb^{3+}). The next step would thus be to consider in detail the redox behavior of the RE^{3+} ions. For that purpose, the 3rd and 4th ionization energies [71] of the RE^{2+} and RE^{3+} ions were considered (Fig. 8). Especially, the 3rd ionization energies are relevant for the electron transfer processes when the redox couples Eu^{2+}/Eu^{3+} and RE^{3+}/RE^{2+} are considered. Indeed, the RE^{2+}/RE^{3+} ionization energies for the Dy^{3+}, Ho^{3+} and Er^{3+} ions are quite similar, but that for Nd^{3+} deviates significantly from this group of RE^{3+} ions which all were found to enhance the persistent luminescence in $Sr_2MgSi_2O_7$:Eu^{2+}. Since the 3rd ionization energy should be related to the depth of the electron trap, the huge energy difference (on the thermal energy scale, of course) between Nd^{3+} and Dy^{3+} is in conflict with their rather similar behavior. Following the somewhat arbitrary method of regrouping the 3rd ionization energies [72] of the RE^{2+} ions (the parallel lines in Fig. 8), the Nd^{3+} energy can be included but the physical meaning of the method is not explained in the original work [72]. It is thus necessary to introduce a systematic relationship between the energies of the $4f^n$ energy levels of the RE^{3+}/RE^{2+} ions and the host band structure which is carried out in the next chapter.

Positions of $4f^n$ levels in the $Sr_2MgSi_2O_7$ host band structure

In the beginning of 2000s, a systematic approach was introduced to define the positions of the $4f^n$ (and $4f^{n-1}5d^1$) ground levels of the RE^{3+}/RE^{2+} ions in the hosts' band structures [73]. Some previous attempts had been made for some of the RE^{3+} and RE^{2+} ions but, at the present stage, the model allows the prediction of any RE^{3+} or RE^{2+} ion level structure in any host starting from only a few data points. However, by achieving such a universal coverage, the accuracy of the model in individual cases may be jeopardized. Nevertheless, this model can be used for the interpretation of many interesting chemical, physical and spectroscopic properties of rare-earths [74]. This model was also suggested [75] to solve the enhancement of persistent luminescence by the RE^{3+} co-dopants in $Sr_2MgSi_2O_7$:Eu^{2+}. It seems now [67] that the defects due to charge compensation originating from the aliovalent substitution of Sr^{2+} by RE^{3+} leads to a multitude of defects overruling the rare-earth ions as traps to store the excitation energy in the charging phase of the persistent luminescence mechanism. As a result, not only one trap *per* a given RE^{3+} co-dopant is observed with thermoluminescence measurements for the Eu^{2+},RE^{3+}-co-doped $Sr_2MgSi_2O_7$ materials, but several of them (Fig. 9). Furthermore, it is difficult to differentiate the rare-earth traps from the charge com-

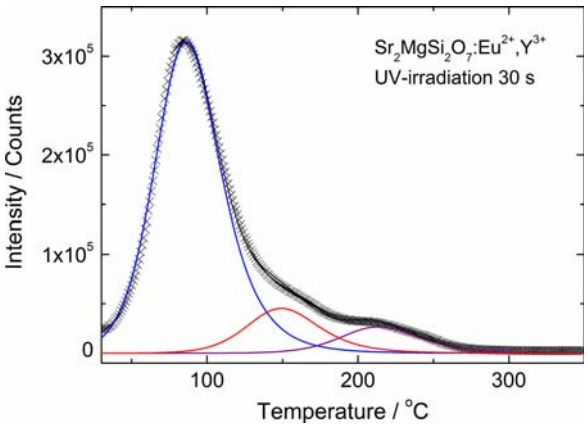

Fig. 9 (color online). The thermoluminescence glow curve of the $Sr_2MgSi_2O_7$: Eu^{2+},Y^{3+} persistent luminescence material indicating more than one glow peak and thus more than one trap. The glow curves were deconvoluted with the program TLANAL v.1.0.3 [55, 56].

pensating ones [67] – possibly since the defects (being charged species) interact with each other and thus modify their energies.

Despite the problems with accuracy, omission of the charge compensation effects and the fact that no RE^{2+} species (except for Sm^{2+}) has been observed experimentally, remarkable results have been obtained for the rather simple systems with no charge compensation problems, as *e. g.* YVO_4:Ce^{3+},RE^{3+} [76]. Finally, for the persistent luminescence materials such as Eu^{2+},RE^{3+}-co-doped $Sr_2MgSi_2O_7$, no RE^{3+} co-dopant is needed to obtain persistent luminescence – albeit weak (Fig. 7) but at least to some extent. The Eu^{2+},RE^{3+} ↔ Eu^{3+},RE^{2+} redox couples are thus not needed, either.

One important improvement of the ionization potential model (which is, in fact, included into the energy level model) was achieved by recognizing that in real systems the $4f^n$ ground level energies of the Nd^{2+}, Dy^{2+}, Ho^{2+}, and Er^{2+} ions are very close to each other (Fig. 10) and could explain the similar behavior of Nd^{3+} and Dy^{3+} co-doping. The accuracy of the model, being of the order of 0.5 eV, is not, however, sufficient to draw more quantitative conclusions on the Eu^{2+},RE^{3+}-co-doped $Sr_2MgSi_2O_7$ system. It was thus recognized that a more tangible model with a possibility to measure experimentally the basic parameters is needed to explain the enhancement of persistent luminescence in the Eu^{2+},RE^{3+}-co-doped $Sr_2MgSi_2O_7$ materials.

Tuning the host's band gap

The essential parts of the mechanism [66] for the persistent luminescence from the materials based on doping with Eu^{2+} (Fig. 11) are nowadays widely accepted. The importance of the band gap energy, the position of the Eu^{2+} $^8S_{7/2}$ ground level in the band structure of the host as well as the electrons as charge carriers (the position of the $4f^6 5d^1$ levels close to or within the host's CB) and their trapping in electron traps close to the bottom of the host's CB is well established, and these details are ready to be used in the design of new, more efficient persistent luminescence materials. Thus, only the role of the RE^{3+} co-dopant is left to be answered. Since the previous models (*cf.* above) have all so far failed to various extent, a new approach was adopted in this contribution: tuning the band gap of the host. Density Functional Theory (DFT) calculations [77] have shown that the valence band of $Sr_2MgSi_2O_7$ is composed almost exclusively of the oxygen $2p$ orbitals and the bottom of the conduction band of $Sr_2MgSi_2O_7$ mainly of the Sr($4d$) orbitals, whereas the Si and Mg orbitals are far off in the conduction band. Although the $4f^7$ ground level of Eu^{2+} is in the host's band gap, the other $4f^7$ and $4f^6 5d^1$ levels are in the conduction band. This is also the case for the RE^{3+} and especially for the RE^{2+} ions. DFT calculations have also shown that the oxygen vacancy states are close to the bottom of the host's CB [77]. Since they are associated with oxygen only, their absolute positions in the band gap can be consid-

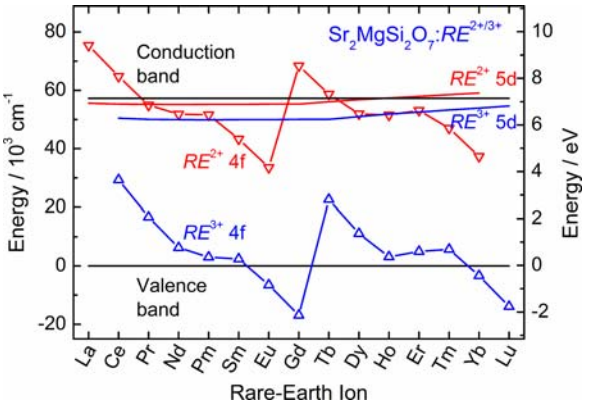

Fig. 10 (color online). The ground level positions of the $4f^n$ (and $4f^{n-1}5d^1$) electron configurations for the RE^{2+} and RE^{3+} ions *vis-à-vis* the $Sr_2MgSi_2O_7$ host band structure (calculated following the method presented earlier [73]).

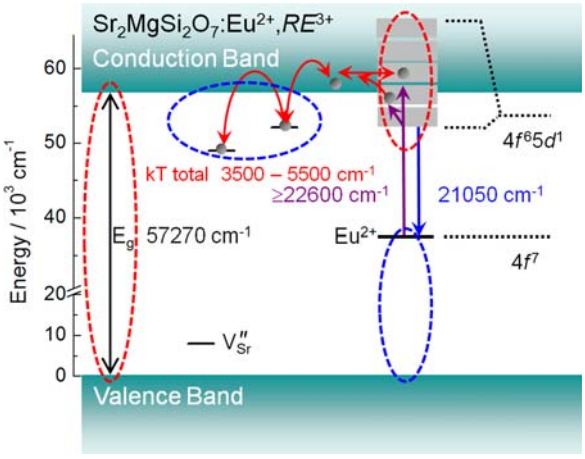

Fig. 11 (color online). The persistent luminescence mechanism for the $Sr_2MgSi_2O_7$:Eu^{2+},RE^{3+} materials (modified from ref. [66]).

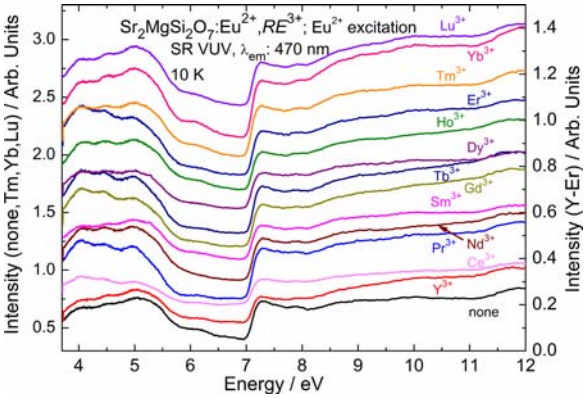

Fig. 12 (color online). The SR UV-VUV excitation spectra of Eu^{2+} in $Sr_2MgSi_2O_7$:Eu^{2+},RE^{3+} persistent luminescence materials at 10 K.

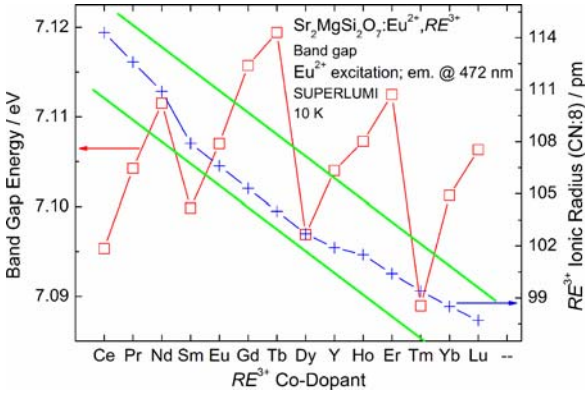

Fig. 13 (color online). The band gap energy (E_g) *i. e.* the peak energy of the 1st derivative of the host's valence to conduction band edge in the UV-VUV synchrotron radiation excitation spectra of $Sr_2MgSi_2O_7$:Eu^{2+},RE^{3+}. The ionic radii for the RE^{3+} species (for the coordination number 8) [58] are presented as well.

ered as constant. Thus the possibility to probe the band gap energy with the change of the RE^{3+} co-dopant became a reality.

The basic idea of the model was to "freeze" the energy level system of the entire Eu^{2+}-doped $Sr_2MgSi_2O_7$ except for the effect of the RE^{3+} co-dopants. The latter were thus the only part of the system to modify the position of the bottom of the system's CB. Since the calculation of this effect with DFT methods quickly proved very difficult or presently even impossible, the possibility to measure experimentally the effect of different RE^{3+} co-dopants on the band gap energy was taken into account as the sole alternative. The following experimental difficulties were considered important: the band gap energy of $Sr_2MgSi_2O_7$ is *ca.* 7.1 eV which required VUV measurements (Fig. 12). The RE^{3+} doping level was only 1 mole-% of the strontium amount, thus the modification of the band gap energy may be rather small. As an indication of the magnitude of this effect, the trap energies due to RE^{3+} co-doping – calculated from the TL measurements [67] – differed by several hundred meV, and thus the resolution of the SUPERLUMI apparatus (0.02 nm) was considered sufficient to try the experiments. Previous measurements have shown that no exciton fine structure was present in the vicinity of the fundamental edge of the $Sr_2MgSi_2O_7$ host and thus perturbation-free results could be expected. To achieve the required accuracy, the measurement of the excitation spectra of Eu^{2+} requires the treatment of the spectral data with the 1st (or even the 2nd) derivative to obtain exact energy values.

The measurement of the excitation spectra of the Eu^{2+},RE^{3+}-co-doped $Sr_2MgSi_2O_7$ in the SR VUV range at 10 K produced very similar spectra, indicating the host edge at *ca.* 7.1 eV (Fig. 12). Below 7 eV one can observe the $4f^7 \rightarrow 4f^6 5d^1$ bands of Eu^{2+} which are not smoothed down at 10 K because no persistent luminescence is present due to the absence of sufficient thermal energy. This was one of the reasons for carrying out the measurements at 10 K since at higher temperatures the persistent luminescence makes the spectra difficult to interpret or, alternatively, very time consuming and inaccurate to measure. The host edge at *ca.* 7.1 eV is a neat step function with very little fine structure and free of exciton bands but still requires the use of the 1st derivative curve to obtain exact energy values (not shown here).

The measured band gap energies (Fig. 13) at 10 K varied within a rather small energy range, from 7.09 to 7.12 eV, the difference corresponding to *ca.* 250 cm^{-1} – approximately equal to the thermal energy at room temperature. Because of the low doping level of the RE^{3+} ions (1 mole-%), one could not expect very different results. As to the accuracy of the results, the resolution of the apparatus being 0.02 nm (at *ca.* 175 nm this equals to *ca.* 7 cm^{-1} (0.9 meV) or, in relative measures, $\Delta E/E = 1 \times 10^{-4}$), the results can be considered very reliable. Of course, some error is always introduced. At the first glance, the energy gap values produced a weird zig-zag curve (Fig. 13), and no systematics could be observed in the band gap values. How-

ever, after applying a similar regrouping of the energy values as previously [72], the Nd^{3+}, Dy^{3+} and Tm^{3+} ions (Ho^{3+} is not too far, either) could be separated with two parallel lines into a group. This group has approximately the band gap energy to create trap depths suitable for enhancing the persistent luminescence of the Eu^{2+}-doped $Sr_2MgSi_2O_7$. In contrast to the previous model based on the ionization energies [72], where the orientation (slope) of the limiting lines could not be justified, in the present model, one can observe an excellent co-linearity with the evolution of the RE^{3+} ion size. This could suggest that, after all, the charge density of the RE^{3+} ions plays a role in the tuning of the band gap energy of $Sr_2MgSi_2O_7$. This possibility should, however, be studied in detail with *e. g.* DFT calculations which can probe details that are impossible to observe experimentally.

The band gap energy values revealed that evidently the gap energies below the lower line are too low and produce too shallow traps for good room temperature persistent luminescence. Similarly, the gap energies above the upper line produce too deep traps. In addition to explaining the enhancement of persistent luminescence of Eu^{2+},RE^{3+}-co-doped $Sr_2MgSi_2O_7$ at room temperature, this method can predict the optimum temperature for the application of a particular material.

Conclusions

Tetragonal Eu^{2+},RE^{3+}-co-doped $Sr_2MgSi_2O_7$ persistent luminescence materials could be prepared with high purity. The effect of different RE^{3+} co-dopants was drastically different in the enhancement of the persistent luminescence and, in general, the typical RE^{3+} ions with stable +3 valence such as Nd^{3+}, Dy^{3+} and Ho^{3+} gave the best results. However, Sm^{3+}- and Yb^{3+}-co-doping resulted in close to total quenching of persistent luminescence probably due to the easy reduction of these ions to the divalent state. As to the mechanism of enhancement, the aliovalent substitution of the Sr^{2+} host cation with the RE^{3+} co-dopant leads to charge compensation defects that override the effect of the RE^{3+} ions acting as electron traps. The ionization potential and energy level models proved to be too simple and/or inaccurate to predict the enhancement of the persistent luminescence in Eu^{2+},RE^{3+}-co-doped $Sr_2MgSi_2O_7$. The experimental determination of the band gap energy for $Sr_2MgSi_2O_7$ materials with different RE^{3+} co-doping gave good results that explain the enhancement of the persistent luminescence. More work is needed to refine the model, however.

Experimental Section

Preparation

The polycrystalline $Sr_2MgSi_2O_7$:Eu^{2+},RE^{3+} (*RE*: Y, La–Lu, excluding Pm and Eu) materials were prepared by a solid-state reaction between stoichiometric amounts of $SrCO_3$ (Merck, Pro Analysi), $Mg(NO_3)_2{\cdot}6H_2O$ (Merck, Pro Analysi), fumed SiO_2 (Sigma, 99.8 %) and rare-earth oxides (different manufacturers; 99.9 – 99.99 %) using heating at 700 °C for 1 h followed by annealing at 1350 °C for 10 h in a reducing $N_2 + 10\%$ H_2 gas sphere. The materials were doped and co-doped with 1 mole-% of both the Eu^{2+} and RE^{3+} ions calculated on the strontium amount.

Characterization

The crystal structures and phase purities of the materials were analyzed by powder X-ray diffraction (PXD) measurements. The patterns were collected at room temperature between 4 and 100° (in 2θ) with a Huber G670 image plate Guinier camera (CuK_{α_1} radiation, $\lambda = 1.5406$ Å). The data collection time was 30 min. The asymmetry of the diffraction reflections (Fig. 3) is due to the apparatus used. For Rietveld refinements, *e. g.*, this effect can still be successfully compensated.

The TL glow curves were measured with an upgraded Risø TL/OSL-DA-12 system using a constant heating rate of 5 °C s^{-1} in the temperature range from 25 to 400 °C. The global TL emission from UV to 650 nm was monitored. Prior to the TL measurements, the samples were irradiated with a combination of Philips TL 20 W/05 (emission maximum at 360 nm) and TL 20 W/03 (420 nm) UV lamps for 30 s. A delay of 3 min was used between the irradiation and the measurement. The analysis of the TL glow curves was carried out by the deconvolution of the TL curves with the program TLANAL v.1.0.3 [55, 56]. The bands were considered to be of the second-order kinetics because of their symmetrical shape.

The persistent luminescence spectra were recorded at room temperature with a Varian Cary Eclipse spectrometer. Prior to the measurements, the materials were irradiated for 5 min with UV radiation at 254 nm. The delay between the irradiation and the measurement was 1 and 10 min.

The UV-VUV excitation spectra of $Sr_2MgSi_2O_7$:Eu^{2+},RE^{3+} were recorded between 80 and 330 nm using the SUPERLUMI (beamline I) synchrotron radiation facility of HASYLAB (Hamburger Synchrotronstrahlungslabor) at DESY (Deutsches Elektronen-Synchrotron, Hamburg, Germany). The polycrystalline materials were mounted

on the cold finger of a liquid He flow cryostat, and the spectra were recorded at selected temperatures between 10 K and room temperature. The setup consisted of a 2-m McPherson-type primary (excitation) monochromator with a resolution up to 0.02 nm. The UV-VUV excitation spectra were corrected for the variation in the incident flux of the excitation beam using the excitation spectrum of sodium salicylate as a standard. The emission spectra were recorded at selected temperatures with an ARC SpectraPro-308i monochromator equipped with a SSL CCD camera.

Acknowledgement

Financial support is acknowledged from the Academy of Finland, projects "Energy Storage Luminophors 2" (134459/2009) and "Novel Rare Earth Optical Sensors and Materials" (271149/2012), as well as from CNPq, inct-INAMI, FAPESP, Coimbra Group, and CAPES (Brazil). The DFT calculations were carried out using the supercomputing resources of the CSC IT Center for Science (Espoo, Finland). The study was also supported by the Academy of Finland research mobility agreements with the Academy of Sciences of the Czech Republic as well as the Czech research project AVOZ10100521. The synchrotron radiation study was supported by the European Community's Seventh Framework Programme (FP7/2007-2013) under grant agreement no. 312284. Dr. K. O. Eskola (University of Helsinki, Helsinki, Finland) is acknowledged for the use of the thermoluminescence setup, MSc M. Malkamäki (University of Turku, Turku, Finland) for assistance in the synchrotron measurements, Dr. P. Novák (Academy of Sciences of the Czech Republic, Prague, Czech Republic) for the expertise in DFT calculations and MSc T. Laihinen (University of Turku, Turku, Finland) for participating in writing of the manuscript.

[1] E. N. Harvey, *A History of Luminescence: From the Earliest Times Until 1900*, Amer. Phil. Soc., Philadelphia, PA, **1957**, chapter VIII.
[2] X. Wang, D. Jia in *Phosphor Handbook*, (Eds. S. Shionoya, W. M. Yen, H. Yamamoto), 2nd edition, CRC Press, Boca Raton, FL, **2007**, pp. 793 – 818.
[3] T. Aitasalo, P. Dereń, J. Hölsä, H. Jungner, J.-C. Krupa, M. Lastusaari, J. Legendziewicz, J. Niittykoski, W. Stręk, *J. Solid State Chem.* **2003**, *171*, 114 – 122.
[4] J. Hölsä, *Electrochem. Soc. Interface* **2009**, *18*, 42 – 45.
[5] H. F. Brito, J. Hölsä, T. Laamanen, M. Lastusaari, M. Malkamäki, L. C. V. Rodrigues, *Opt. Mater. Expr.* **2012**, *2*, 371 – 381.
[6] Fortunius Licetus, *Litheosphorus Sive de Lapide Bononiens*, Università di Bologna, Bologna, **1640**.
[7] M. Lastusaari, T. Laamanen, M. Malkamäki, K. O. Eskola, A. Kotlov, S. Carlson, E. Welter, H. F. Brito, M. Bettinelli, H. Jungner, J. Hölsä, *Eur. J. Miner.* **2012**, *24*, 885 – 890.
[8] Y. Murayama in *Phosphor Handbook*, (Eds.: S. Shionoya, W. M. Yen, H. Yamamoto), 2nd edition, CRC Press, Boca Raton, FL, **2007**, pp. 789 – 792.
[9] H. Yamamoto, T. Matsuzawa, *J. Lumin.* **1997**, *72 – 74*, 287 – 289.
[10] K. Van den Eeckhout, P. F. Smet, D. Poelman, *Materials* **2010**, *3*, 2536 – 2566.
[11] T. Maldiney, A. Lecointre, B. Viana, A. Bessière, M. Bessodes, D. Gourier, C. Richard, D. Scherman, *J. Am. Chem. Soc.* **2011**, *133*, 11810 – 11815.
[12] Z. Pan, Y.-Y. Lu, F. Liu, *Nat. Mater.* **2012**, *11*, 58 – 63.
[13] L. C. V. Rodrigues, J. Hölsä, M. Lastusaari, M. C. F. C. Felinto, H. F. Brito, *J. Mater. Chem. C* **2014** (DOI: 10.1039/C3TC31995D).
[14] D. Jia, X. J. Wang, W. M. Yen, *Chem. Phys. Lett.* **2002**, *363*, 241 – 244.
[15] J. Trojan-Piegza, E. Zych, J. Hölsä, J. Niittykoski, *J. Phys. Chem. C* **2009**, *113*, 20493 – 20498.
[16] L. C. V. Rodrigues, H. F. Brito, J. Hölsä, R. Stefani, M. C. F. C. Felinto, M. Lastusaari, T. Laamanen, L. A. O. Nunes, *J. Phys. Chem. C* **2012**, *116*, 11232 – 11240.
[17] Y. Cong, B. Li, B. Lei, W. Li, *J. Lumin.* **2007**, *126*, 822 – 826.
[18] J. M. Carvalho, L. C. V. Rodrigues, J. Hölsä, M. Lastusaari, L. A. O. Nunes, M. C. F. C. Felinto, O. L. Malta, H. F. Brito, *Opt. Mater. Expr.* **2012**, *2*, 331 – 340.
[19] T. Lin, Z. Tang, Z. Zhang, X. Wang, J. Zhang, *J. Mater. Sci. Lett.* **2001**, *20*, 1505 – 1506.
[20] Z. Qi, C. Shi, M. Liu, D. Zhou, X. Luo, J. Zhang, Y. Xie, *Phys. Status Solidi a* **2004**, *201*, 3109 – 3112.
[21] S. Carlson, J. Hölsä, T. Laamanen, M. Lastusaari, M. Malkamäki, J. Niittykoski, R. Valtonen, *Opt. Mater.* **2009**, *31*, 1877 – 1879.
[22] T. Aitasalo, J. Hassinen, J. Hölsä, T. Laamanen, M. Lastusaari, M. Malkamäki, J. Niittykoski, P. Novák, *J. Rare Earths* **2009**, *27*, 529 – 538.
[23] Y. Z. Li, Y. H. Wang, Z. H. Zhang, W. J. Liu, *Electrochem. Solid State Lett.* **2006**, *9*, J37–J39.
[24] Y. Chen, B. Liu, M. Kirm, Z. Qi, C. Shi, M. True, S. Vielhauer, G. Zimmerer, *J. Lumin.* **2006**, *118*, 70 – 78.
[25] D. Jia, D. N. Hunter, *J. Appl. Phys.* **2006**, *100*, 113125.
[26] C. S. Shi, Y. B. Fu, B. Liu, G. B. Zhang, Y. H. Chen, Z. M. Qi, X. X. Luo, *J. Lumin.* **2007**, *122*, 11 – 13.
[27] H. M. Ji, G. J. Xie, Y. Lv, H. X. Lu, *J. Sol-Gel Sci. Techn.* **2007**, *44*, 133 – 137.
[28] M. Zhang, J. Wang, W. J. Ding, Q. H. Zhang, Q. Su, *Opt. Mater.* **2007**, *30*, 571 – 578.

[29] F. L. Song, D. H. Chen, Y. H. Yuan, *J. Alloys Compd.* **2008**, *458*, 564 – 568.
[30] W. Pan, G. L. Ning, X. Zhang, J. Wang, Y. Lin, J. W. Ye, *J. Lumin.* **2009**, *128*, 1975 – 1979.
[31] Y. C. Xu, D. H. Chen, *Ceram. Int.* **2008**, *34*, 2117 – 2120.
[32] Y. Q. Li, Y. H. Wang, Y. Gong, X. H. Xu, *J. Electrochem. Soc.* **2009**, *156*, J77–J88.
[33] H. W. Zhang, N. Terasaki, H. Yamada, C. N. Xu, *Int. J. Mod. Phys. B* **2009**, *23*, 1028 – 1033.
[34] H. W. Zhang, N. Terasaki, H. Yamada, C. N. Xu, *Jpn. J. Appl. Phys.* **2009**, *48*, 04C109.
[35] W. Pan, G. L. Ning, J. Wang, Y. Lin, J. W. Ye, *J. Lumin.* **2009**, *129*, 584.
[36] Y. Q. Li, Y. H. Wang, X. H. Xu, Y. Gong, *J. Lumin.* **2009**, *129*, 1230 – 1234.
[37] G. J. Talwar, C. P. Joshi, S. V. Moharil, S. M. Dhopte, P. L. Muthal, V. K. Kondawar, *J. Lumin.* **2009**, *129*, 1239 – 1241.
[38] H. Y. Wu, Y. H. Hu, Y. H. Wang, B. D. Zeng, Z. F. Mou, L. Y. Deng, W. Xie, *J. Alloys Compd.* **2009**, *486*, 549 – 553.
[39] S. J. Han, S. M. Lee, S. H. Sohn, *Mol. Cryst. Liq. Cryst.* **2010**, *531*, 96 – 100.
[40] X. H. Chen, Y. H. Hu, Y. H. Wang, *J. Nanosci. Nanotechn.* **2010**, *10*, 1865 – 1870.
[41] H. Y. Wu, Y. H. Hu, Y. H. Wang, C. J. Fu, *J. Alloys Compd.* **2010**, *497*, 330 – 335.
[42] H. Y. Wu, Y. H. Hu, Y. H. Wang, C. J. Fu, *Mater. Sci. Eng. B* **2010**, *172*, 276 – 282.
[43] Z. G. Xia, J. Y. Sun, L. B. Liao, H. Y. Du, *J. Rare Earths* **2010**, *28*, 874 – 877.
[44] F. Yoshimura, K. Nakamura, F. Wakai, M. Hara, M. Yoshimoto, O. Odawara, H. Wada, *Appl. Surf. Sci.* **2011**, *257*, 2170 – 2175.
[45] H. Y. Wu, Y. H. Hu, X. J. Wang, *Radiat. Meas.* **2011**, *46*, 591 – 594.
[46] H. Y. Wu, Y. H. Hu, L. Chen, X. J. Wang, *Mater. Lett.* **2011**, *65*, 2676 – 2679.
[47] H. Y. Wu, Y. H. Hu, B. D. Zeng, Z. F. Mou, L. Y. Deng, *J. Phys. Chem. Solids* **2011**, *72*, 1284 – 1289.
[48] T. Kim, Y. Kim, S. Kang, *Appl. Phys. B* **2012**, *106*, 1009 – 1013.
[49] M. T. Zheng, X. B. Chen, B. F. Lei, Y. Xiao, R. Liu, H. R. Zhang, H. W. Dong, Y. L. Liu, X. T. Liu, *ECS Solid State Lett.* **2013**, *2*, R19–R22.
[50] K. H. Kwon, W. B. Im, D. Y. Jeon, *J. Nanosci. Nanotechn.* **2013**, *13*, 4079 – 4083.
[51] Y. Q. Zhai, J. Chen, L. L. Wang, J. Ma, Z. C. Hu, *Asian J. Chem. A* **2013**, *25*, 6247 – 6250.
[52] D. Poelman, P. F. Smet, *Opt. Express* **2010**, *18*, 26293 – 26299.
[53] Y. Ochi, *Mater. Res. Bull.* **2006**, *41*, 1825 – 1834.
[54] J. Hölsä, H. Jungner, M. Lastusaari, J. Niittykoski, *J. Alloys Compd.* **2001**, *323 – 324*, 326 – 330.
[55] K. S. Chung, H. S. Choe, J. I. Lee, J. L. Kim, S. Y. Chang, *Radiat. Prot. Dosim.* **2005**, *115*, 343 – 349.
[56] K. S. Chung, TLANAL (version 1.0.3), TL Glow Curve Analyzer, Korea Atomic Energy Research Institute and Gyeongsang National University (Korea) **2008**.
[57] International Centre for Diffraction Data (ICDD), Powder Diffraction File PDF-4+, entries 04-009-1842 ($Sr_2MgSi_2O_7$) and 01-078-5582 ($Sr_3MgSi_2O_8$), **2012**.
[58] R. D. Shannon, *Acta Crystallogr.* **1976**, *A32*, 751 – 767.
[59] A. R. Denton, N. W. Ashcroft, *Phys. Rev. A* **1991**, *43*, 3162 – 3164.
[60] I. D. Brown, *The Chemical Bond in Inorganic Chemistry: The Bond Valence Model*. IUCr Monographs in Crystallography 12, Oxford Science, Oxford, **2002**.
[61] M. Lastusaari, *Rietveld Refinement of the Crystal Structure of $Sr_2MgSi_2O_7$:Eu^{2+}*, University of Turku, Turku, **2006** (unpublished).
[62] M. Kimata, N. Ii, *N. Jb. Miner. Monat.* **1981**, 1 – 10.
[63] M. Shimizu, M. Kimata, I. Iida, *N. Jb. Miner. Monat. H1* **1995**, 39 – 47.
[64] G. Blasse, W. L. Wanmaker, J. W. ter Vrugt, A. Bril, *Philips Res. Rep.* **1968**, *23*, 189 – 200.
[65] F. A. Kröger, H. J. Vink, *J. Phys. Chem. Solids* **1958**, *5*, 208 – 223.
[66] T. Aitasalo, J. Hölsä, H. Jungner, M. Lastusaari, J. Niittykoski, *J. Phys. Chem. B* **2006**, *110*, 4589 – 4598.
[67] H. F. Brito, J. Hassinen, J. Hölsä, H. Jungner, T. Laamanen, M. Lastusaari, M. Malkamäki, J. Niittykoski, P. Novák, L. C. V. Rodrigues, *J. Therm. Anal. Calorim.* **2011**, *105*, 657 – 662.
[68] T. Aitasalo, P. Dereń, J. Hölsä, H. Jungner, M. Lastusaari, J. Niittykoski, W. Stręk, *Radiat. Meas.* **2004**, *38*, 515 – 518.
[69] L. R. Morss, *Chem. Rev.* **1976**, *76*, 827 – 841.
[70] F. Clabau, X. Rocquefelte, S. Jobic, P. Deniard, M.-H. Whangbo, A. Garcia, T. Le Mercier, *Chem. Mater.* **2005**, *17*, 3904 – 3912.
[71] K. L. Van der Sluis, L. J. Nugent, *J. Chem. Phys.* **1974**, *60*, 1927 – 1930.
[72] G. Ju, Y. Hu, L. Chen, X. Wang, *J. Appl. Phys.* **2012**, *111*, 113508.
[73] P. Dorenbos, *J. Lumin.* **2004**, *108*, 301 – 305.
[74] E. van der Kolk, P. Dorenbos, *Chem. Mater.* **2006**, *18*, 3458 – 3462.
[75] P. Dorenbos, *Phys. Status Solidi B* **2005**, *242*, R7–R9.
[76] P. Dorenbos, A. J. J. Bos, N. R. J. Poolton, *Opt. Mater.* **2011**, *33*, 1019 – 1023.
[77] J. Hölsä, T. Laamanen, M. Lastusaari, P. Novák, *Phys. Procedia* **2012**, *29*, 76 – 85.